

Quasiparticle vanishing driven by geometrical frustration

A. E. Trumper, C. J. Gazza, and L. O. Manuel

*Instituto de Física Rosario (CONICET) and Universidad Nacional de Rosario,
Boulevard 27 de Febrero 210 bis, (2000) Rosario, Argentina*

(Dated: February 12, 2018)

We investigate the single hole dynamics in the triangular $t-J$ model. We study the structure of the hole spectral function, assuming the existence of a 120° magnetic Néel order. Within the self-consistent Born approximation (SCBA) there is a strong momentum and t sign dependence of the spectra, related to the underlying magnetic structure and the particle-hole asymmetry of the model. For positive t , and in the strong coupling regime, we find that the low energy quasiparticle excitations vanish outside the neighbourhood of the magnetic Goldstone modes; while for negative t the quasiparticle excitations are always well defined. In the latter, we also find resonances of magnetic origin whose energies scale as $(J/t)^{2/3}$ and can be identified with string excitations. We argue that this complex structure of the spectra is due to the subtle interplay between magnon-assisted and free hopping mechanisms. Our predictions are supported by an excellent agreement between the SCBA and the exact results on finite size clusters. We conclude that the conventional quasiparticle picture can be broken by the effect of geometrical magnetic frustration.

I. INTRODUCTION

The study of doped antiferromagnets has become a central topic in the area of strongly correlated electrons systems, mainly after Anderson's proposition¹ about the probable existence of non-Fermi liquid behavior once a Mott insulating state is hole-doped. A valuable experiment that gives access to single-particle properties of many-electron systems is the angle resolved photoemission spectroscopy (ARPES). Even though in the last years there has been a rapid pace of developments in ARPES experiments, there are still controversies in many strongly interacting cases, like the cuprates, where the difficulty to distinguish a coherent δ -function peak from an incoherent part of the spectra does not allow a proper interpretation of the available data^{2,3}. A useful microscopic model widely used to describe the low-energy physics involved in photoemission experiments of antiferromagnetic Mott insulators⁴ is the $t-J$ model on the square lattice⁵.

Attention has also been concentrated on triangular Mott insulators. These systems are attractive due to the presence of both, strong correlation and geometrical magnetic frustration, leading to non-conventional behavior. Experimental realizations of such systems are Cs_2CuCl_4 ⁶, the κ family of the organic charge transfer salts $(BEDT-TTF)_2X$ ⁷, and the silicon surfaces K/Si (111):B and SiC(0001)^{8,9}. In a recent publication, Koretsune and Ogata¹⁰ have studied the effect of finite doping in the triangular Heisenberg model. They found that a resonating-valence-bond (RVB) ground state is favored when t is positive, while a Nagaoka's ferromagnetic ground state is stabilized for negative t . More recently, the role of the t sign and frustration has been addressed in the superconductor $NaxCoO_2$ where the Co atoms form the triangular lattice¹¹. These remarkable issues lead us to investigate the spectral function of a hole in a triangular Mott insulator, so as to analyze the consequences of the geometrical frustration and the t sign on

the hole motion. In particular, our aim is to study the existence of quasiparticle (QP) excitations and higher-energy features in the spectral functions. To this purpose, we focus on the hole dynamics in the triangular $t-J$ model, and we solve it using the Lanczos exact diagonalization method and the self-consistent Born approximation (SCBA). In the non-frustrated case, it is known that the SCBA reproduces quite well the exact diagonalization results on small clusters¹² and the angle-resolved photoemission spectroscopy (ARPES) experiments⁴. In particular, the SCBA predicts the existence of a well defined quasiparticle peak (magnetic polaron) at low energies for the whole Brillouin zone (BZ). Furthermore, the SCBA is able to capture finite lifetime resonances above the QP peaks. These resonances have been explained by the string picture since their energies scale as $(J/t)^{2/3}$, as it happens in the Ising limit. In our triangular frustrated case, the presence of the 120° Néel order generates two mechanisms for hole motion in the SCBA effective Hamiltonian, one being tight-binding like (or free) and the other, magnon-assisted. We will show that the t sign tunes the interference between both mechanisms, producing pronounced differences in the low energy as well as in the higher energy region of the spectral functions. For the strong coupling regime, we find an excellent agreement between the SCBA and the exact results on a 21 sites cluster. In the thermodynamic limit, the SCBA spectral functions present a rich structure. Notably, for $t < 0$ a quasiparticle excitation is always defined for all \mathbf{k} of the Brillouin zone, while for $t > 0$ in the strong coupling regime the quasiparticle signal survives only around the Goldstone magnetic wave vectors. By computing the quasiparticle energy scaling with J/t it is possible to get some insight of the magnetic cloud surrounding the hole¹³. We argue that for $t < 0$ the local environment around the hole enhances its AF character, while for $t > 0$ the ferromagnetic character is favored. We find that the single-hole dynamics in the thermodynamic limit behaves in the opposite way as in very small

clusters, like the three-sites problem¹⁰.

Furthermore, for small values of J/t and $t < 0$, higher energy resonances above the quasiparticle peak appear showing a $(J/t)^{2/3}$ energy scaling. Although the triangular $t - J^z$ model is completely different to the square lattice case, we continue identifying these resonances with string-like excitations. For $t > 0$, instead, we do not observe higher energy resonances that can be identified with strings. This behavior observed at higher energies can be also traced back to the particular features of the magnetic environment around the hole mentioned above.

The paper is organized as follows. In section II we obtain the effective Hamiltonian and the one hole properties within the SCBA. In section III we present the results: (IIIA) the comparison between exact and SCBA results in finite size clusters, (IIIB) the quasiparticle features, and (IIIC) the general description of the spectral functions. Finally, in section IV we draw the concluding remarks.

II. T-J MODEL AND SELF CONSISTENT BORN APPROXIMATION

The $t - J$ model is defined as

$$H = -t \sum_{\langle i,j \rangle} (\hat{c}_{i,\sigma}^\dagger \hat{c}_{j,\sigma} + h.c.) + J \sum_{\langle i,j \rangle} \mathbf{S}_i \cdot \mathbf{S}_j, \quad (1)$$

where the first term represents the hopping between nearest neighbors ($\langle i, j \rangle$) of the triangular lattice, with the constraint of no double occupancy, $\hat{c}_{i,\sigma} = c_{i,\sigma}(1 - n_{i,-\sigma})$, and the second term represents the antiferromagnetic (AF) Heisenberg part with $J > 0$.

The study of the single hole motion in an AF requires a correct description of the magnetic low energy sector since the injected hole will couple strongly with these spin excitations. In the literature there is firm numerical¹⁴ and analytical¹⁵ evidence that the triangular Heisenberg antiferromagnet has a 120° Néel order ground state, and that spin wave theory reproduces quite well its low energy behavior¹⁶. So that, we assume an ordered ground state with a magnetic wave vector $\mathbf{Q} = (4\pi/3, 0)$ lying in the $x - z$ plane, and spin waves as the low energy excitations. In order to simplify the calculation we perform a unitary transformation to local spin quantization axis –primed operators– in order to have a ferromagnetic ground state in the z' direction. Then, we use the spinless fermion representation for electrons $\hat{c}_{i\uparrow}^\dagger = h_i^\dagger, \hat{c}_{i\downarrow}^\dagger = h_i S_i^-$, and the Holstein-Primakov representation for spin operators (to order $1/S$) $S_i^{x'} \sim \frac{1}{2}(a_i^\dagger + a_i), S_i^{y'} \sim \frac{i}{2}(a_i^\dagger - a_i), S_i^{z'} = \frac{1}{2} - a_i^\dagger a_i$, where h_i^\dagger creates a spinless hole at site i , and a_i^\dagger creates a spin deviation.

We replace the above expressions in eq. (1) and, after Fourier and Bogoliubov transformations, the effective Hamiltonian results

$$H = \sum_{\mathbf{k}} \epsilon_{\mathbf{k}} h_{\mathbf{k}}^\dagger h_{\mathbf{k}} + \sum_{\mathbf{q}} \omega_{\mathbf{q}} \alpha_{\mathbf{q}}^\dagger \alpha_{\mathbf{q}}$$

$$-t \sqrt{\frac{3}{N}} \sum_{\mathbf{k}, \mathbf{q}} \left[M_{\mathbf{k}\mathbf{q}} h_{\mathbf{k}}^\dagger h_{\mathbf{k}-\mathbf{q}} \alpha_{\mathbf{q}} + h.c. \right] \quad (2)$$

with $\epsilon_{\mathbf{k}} = -t\gamma_{\mathbf{k}}$ and $\omega_{\mathbf{q}} = \frac{3}{2}J\sqrt{(1-3\gamma_{\mathbf{q}})(1+6\gamma_{\mathbf{q}})}$, the bare hole and magnon dispersions, respectively.

$$M_{\mathbf{k}\mathbf{q}} = i(\beta_{\mathbf{k}v-\mathbf{q}} - \beta_{\mathbf{k}-\mathbf{q}u_{\mathbf{q}}})$$

is the bare hole-magnon vertex interaction with the geometric factors $\gamma_{\mathbf{k}} = \frac{1}{3} \sum_{\mathbf{e}} \cos(\mathbf{k} \cdot \mathbf{e})$ and $\beta_{\mathbf{k}} = \sum_{\mathbf{e}} \sin(\mathbf{k} \cdot \mathbf{e})$ (\mathbf{e} 's are the positive vectors to nearest neighbors), and $u_{\mathbf{q}}$ and $v_{\mathbf{q}}$ are the usual Bogoliubov coefficients.

In the Hamiltonian (2) –constant terms related to magnetic energy are omitted– the free hopping hole term implies a finite probability of the hole to move without emission or absorption of magnons. This is a direct consequence of the underlying *non-collinear* magnetic structure. The hole-magnon interaction adds another mechanism for the charge carrier motion which is magnon-assisted. The latter is responsible for the spin-polaron formation when a hole is injected in a non-frustrated antiferromagnet^{12,17}. We will show the existence of a subtle interference between both processes that turns out to be dependent on the t sign. An important quantity that allows us to study the interplay between such processes is the retarded hole Green function that is defined as $G_{\mathbf{k}}^h(\omega) = \langle AF | h_{\mathbf{k}} \frac{1}{(\omega + i\eta^+ - H)} h_{\mathbf{k}}^\dagger | AF \rangle$, where $|AF\rangle$ is the undoped antiferromagnetic ground state with a 120° Néel order. In the SCBA $|AF\rangle$ is the spin wave AF ground state, and after neglectation of the crossing diagrams, the Dyson's equation for the self energy at zero temperature results

$$\Sigma_{\mathbf{k}}(\omega) = \frac{3t^2}{N_s} \sum_{\mathbf{q}} \frac{|M_{\mathbf{k}\mathbf{q}}|^2}{\omega - \omega_{\mathbf{q}} - \epsilon_{\mathbf{k}-\mathbf{q}} - \Sigma_{\mathbf{k}-\mathbf{q}}(\omega - \omega_{\mathbf{q}})}.$$

We have solved numerically this self-consistent equation for $\Sigma_{\mathbf{k}}(\omega)$, and calculated the hole spectral function $A_{\mathbf{k}}(\omega) = -\frac{1}{\pi} \text{Im} G_{\mathbf{k}}^h(\omega)$, and the quasiparticle (QP) weight $z_{\mathbf{k}} = \left(1 - \frac{\partial \Sigma_{\mathbf{k}}(\omega)}{\partial \omega}\right)^{-1} |_{E_{\mathbf{k}}}$, where the QP energy is given by $E_{\mathbf{k}} = \Sigma_{\mathbf{k}}(E_{\mathbf{k}})$.

III. RESULTS

A. Exact and SCBA comparison

We have computed the one hole spectral function $A_{\mathbf{k}}(\omega)$ using the Lanczos exact diagonalization method (ED) and the SCBA on finite size clusters. To test the reliability of the SCBA predictions we have compared both techniques on the $N = 21$ sites cluster, which preserves the spatial symmetries of the infinite triangular lattice¹⁴. In general, we have found a good agreement between ED and SCBA results for all momenta of the BZ and for $J/|t| \lesssim 1$. In Fig. 1 we show the spectral functions at three representative \mathbf{k} points of the BZ (see

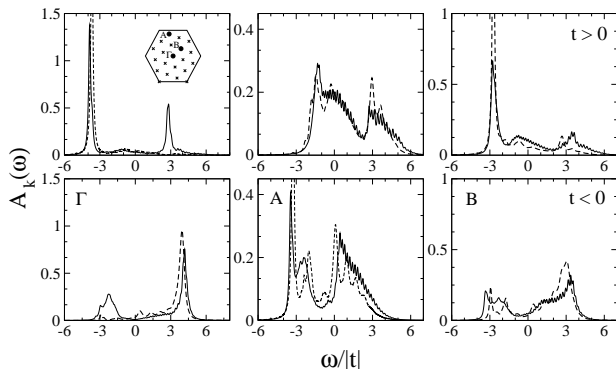


FIG. 1: Spectral functions versus frequency for $J/|t| = 0.4$ and $N = 21$ for momenta $\Gamma = (0, 0)$, $A = \frac{4\pi}{N}(-1, 3\sqrt{3})$ and $B = \frac{4\pi}{N}(2, \sqrt{3})$. \mathbf{k} shown as filled circles in the inset (the crosses represent the other momenta). The upper (lower) panel displays the results for positive (negative) t . The solid and dashed lines are the exact and SCBA results, respectively. $\eta = 0.1$ and $\omega = 10000$ has been used.

inset Fig. 1) in the strong coupling regime, $J/|t| = 0.4$, and for both signs of the transfer integral t .

The exact structure of the spectral functions strongly depends on the momentum because the hole strongly scatter off antiferromagnetic fluctuations⁵. Furthermore, the geometrical frustration is manifested in a marked dependence of the spectral function with the t sign. Remarkably, the SCBA reproduces very well these exact results in the whole range of energies. In some cases from the scale of the figure it cannot be clearly distinguished a quasiparticle peak at low energies. By decreasing η^+ appropriately we have checked, however, the existence of a QP peak for all \mathbf{k} of the BZ. In particular, for negative (positive) t the $\mathbf{k} = \mathbf{A}$ ($\mathbf{k} = \mathbf{\Gamma}$) point becomes the momentum of the quasiparticle ground state. The energy of the hole can be splitted in two contributions: $E^h \equiv E_{N-1} - E_N^{gs} = E_{loc}^h + E_{deloc}^h$, where $E_{loc}^h = E_{N-1}^{t=0} - E_N^{gs}$ is the energy of the localized hole, and $E_{deloc}^h = E_{N-1} - E_{N-1}^{t=0}$ is the energy gain due to delocalization of the hole¹⁸. As the SCBA does not take into account the localized hole energy we have shifted the exact energy spectra by an amount $E_{loc}^h = -0.5686J$ for $N = 21$ in order to make a proper comparison with the SCBA results. The agreement between both techniques is similar to that found in the 4×4 square lattice besides the presence of stronger antiferromagnetic fluctuations in our frustrated case. It was shown that this agreement is a consequence of the small leading nonzero contribution to the self energy from the crossing diagrams¹⁹.

B. Quasiparticle

The momentum and the t sign dependence of the spectra aforementioned is strengthened in the thermodynamic limit. In particular, we observe important dif-

ferences in the quasiparticle weight $z_{\mathbf{k}}$ through the BZ under the change of t sign. Using lattice sizes up to $N = 2700$ we have extrapolated the results to the thermodynamic limit. In Fig.2 we show the values of $z_{\mathbf{k}}$ as a function of J/t for representative points along high symmetry axes of the BZ. The most salient feature we have

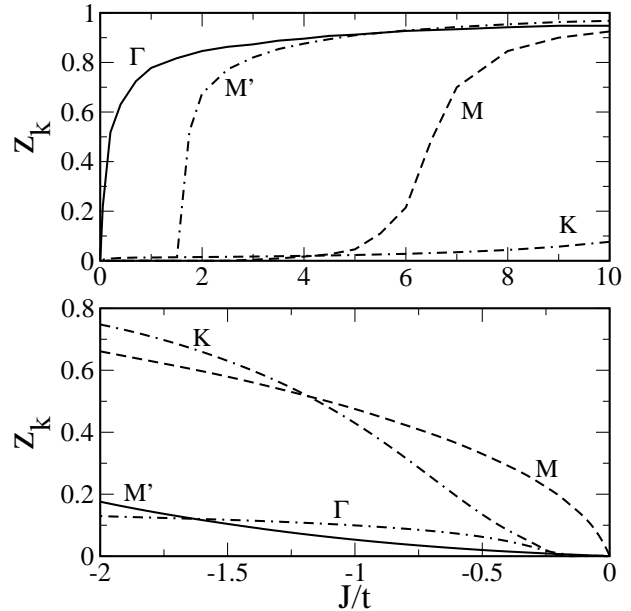


FIG. 2: Quasiparticle weight vs J/t . Upper (lower) panel is for $t > 0$ ($t < 0$). The location of the Γ , M' , K , M is displayed in Fig. 3

obtained is the vanishing of the quasiparticle weight at some momenta for positive t . At the M and M' points $z_{\mathbf{k}} = 0$ below $J/t \sim 2.5$ and 1.5 , respectively. It is worth noticing the robustness and then the rapid decay to zero of $z_{M'}$ as $J/t \rightarrow 1.5$. A similar behavior has the QP signal at Γ , the ground state momentum, but it goes to zero only when $J/t \rightarrow 0$. Finally, the QP signal is very weak, but finite, at the magnetic wave vector K for all the J/t range studied; for instance, $z_{\mathbf{k}} \sim 0.008$ when $J/t = 10$. Surprisingly, for $J \gg t$, z_K does not seem to approach one as it turns out in the square lattice case¹². The non existence of quasi-particle excitations is a striking manifestation of the strong interference between the free and magnon-assisted hopping processes, tuned by the t sign. For the strong coupling regime and a large region of the BZ, the coherence of the QP is lost because of the quite different group velocities of the spin fluctuation and the tight binding hole motion, suggesting the likelihood of a spin-charge separation scenario^{1,3,20} for the triangular $t - J$ model.

On the other hand, for negative t the quasiparticle weight is finite for all momenta and for $J/t \neq 0$. This behavior is similar to the one found in the non-frustrated case¹². It is interesting to note that now the QP ground state momentum is M (K) for $J/|t| \leq 1.2$ ($J/|t| > 1.2$). The spectral weight of the QP becomes the most robust

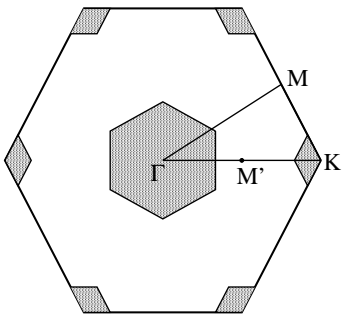


FIG. 3: Triangular Brillouin zone. The shaded areas correspond to the regions where the QP weight is finite for $J/|t| = 0.4$ and positive t .

for the ground state momenta. The interchange in the \mathbf{k} dependence of the QP weight, evidenced in a comparison between both panels of Fig. 2, could be thought as a remnant of the particle-hole symmetry that shifts the momenta by \mathbf{Q} under t sign reversal.

In Fig. 3 the shaded areas correspond to the regions where the QP weight is finite for $J/|t| = 0.4$ and positive t . There is no QP signal for momenta outside the neighborhood of the magnetic Goldstone modes ($\mathbf{k} = \mathbf{0}, \mathbf{Q}$). The presence of QP signal in the non-equivalent vertices of the BZ is an artifact of the used approximation: the spin wave magnetic ground state has a definite chirality (\mathbf{Q}), but our vertex interaction does not discriminate between $\pm\mathbf{Q}$, resulting the whole spectral function degenerate in both momenta. The shaded areas share the same symmetries with the triangular magnetic Brillouin zone. We have noted that as $J/t \rightarrow 0$ they shrink to the magnetic Goldstones modes. Conversely, when $J/t \geq 2.5$ there is a finite QP weight anywhere and therefore, the full BZ becomes shaded. For the particular value $J/|t| = 2$, the QP weight vanishes only around the M point, as it is displayed by the solid line of Fig. 4. This figure also shows the strong \mathbf{k} dependence of the QP weight for both t signs. Again, a signature of the remnant particle-hole symmetry mentioned above is evidenced: the dashed line ($t < 0$) resembles the solid one ($t > 0$) shifted by the wave vector \mathbf{Q} . In a previous work the hole dynamics in a triangular antiferromagnet has already been studied using the SCBA²¹, but the vanishing of the quasiparticle weight for positive t has been overlooked. Our findings, however, are supported by a detailed and careful treatment of the parameters involved: the convergence factor η , the extrapolation to the thermodynamic limit of the cluster sizes N , and the number of frequencies ω ^{19,22}.

By computing the quasiparticle energy scaling with J/t it is possible to get some insight of the magnetic cloud surrounding the hole¹³. It is known that for a ferromagnetic polaron the QP energy scales as $\epsilon \sim (J/t)^{0.5}$, while for an AF polaron it follows a $\epsilon \sim (J/t)^{0.66}$ dependence. In our case we have estimated a $\epsilon \sim (J/t)^\alpha$ scaling, being $\alpha \sim 0.55$ (~ 0.65) for positive (negative) t in the range

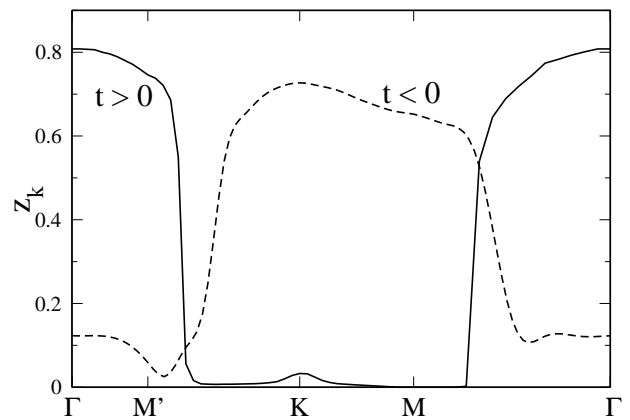


FIG. 4: Quasiparticle weight along the $\Gamma - M' - K - M$ path (see Fig. 3) Solid line is for positive t and dashed line for negative t .

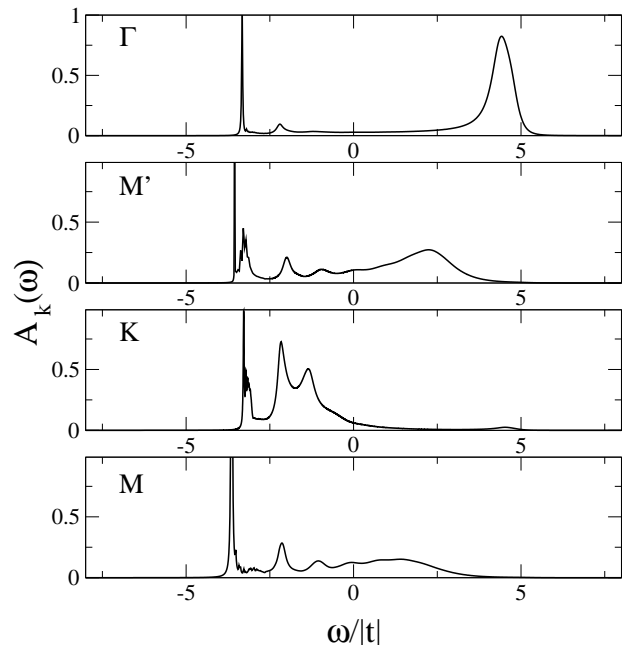


FIG. 5: Spectral function for the Γ, M', K, M points of the Brillouin zone for $J/|t| = 0.4$ and negative t .

$J/|t| \lesssim 0.1$. A possible interpretation of such results is the following: the non-collinear short range magnetic correlations around the hole can be thought as a superposition of ferro and AF correlations, and then for $t < 0$ the local environment around the hole enhances its AF character, while for $t > 0$ the ferromagnetic character is favored. It should be noticed that the opposite behavior holds in a simple toy model consisting of a three-sites $t - J$ model with one hole¹⁰. Actually, we have checked that for cluster sizes smaller than $N = 21$, this behavior is reversed. For instance, for $N = 12$, $\alpha \sim 0.57$ for positive t while for negative t it turns out $\alpha \sim 0.44$.

C. Spectral function structure

In this section we discuss the main features of the spectral functions in the thermodynamic limit. The arising structures can be traced back to the two hole motion processes present in the effective Hamiltonian (2). The spectral functions at the Γ , M' , K and M points are displayed in Fig. 5 for $J/|t| = 0.4$ and negative t . The spectra extend over a frequency range of order $9t$; that is, the non-interacting electronic energy scale. It is possible to discern two distinct regions: a low energy sector of magnetic origin (magnon-assisted), and a high energy sector with a broad resonance related to the free hopping process. This resonance, located at an energy near $\epsilon_{\mathbf{k}}$, has a finite lifetime of order $\sim 4J$ and a dispersion of order t . Furthermore, the low energy sector consists of a quasiparticle peak and higher energy resonances with a narrow dispersion of order J as the momentum varies. We will show below that the latter resonances can be identified with string excitations. At Γ and M' both sectors are well separated in energy, while at K and M they overlap. From Γ to M there is a spectral weight transfer from the high energy sector to the QP peak as it can be also noticed quantitatively in the lower panel of Fig. 2. In Fig. 6 we show the magnetic resonances above the QP peak for $J/|t| = 0.1$ (at the ground state momentum M). We choose this particular parameter value in order to make them more visible, although they are clearly noticeable for $J/t \leq 0.5$. In the inset it is shown the energies of the first three resonances *versus* $(J/t)^{2/3}$. The linear dependence of their energies allow us to associate these resonances with string excitations of a hole confined by an effective linear potential of order J^5 .¹⁹ As we have previously stated, there is a dynamical enhancement of the AF environment around the hole when t is negative, and this effect is the responsible for the strong confining potential seen by the hole, like in the square lattice case.

For positive t (Fig. 7), the low energy sector consists of a QP peak, when it exists (Γ and K), and there is no signature of string-like excitations. This result is a manifestation of the ferromagnetic-like environment around the hole, pointed out before, for this t sign. Again the high energy sector has a broad bandwidth of order $\sim 9t$. It is important to notice that at the ground state momentum Γ the QP is very robust, being the only relevant feature of the spectral function. Otherwise, at M' and M the spectral functions are almost structureless.

IV. CONCLUDING REMARKS

We have studied the effect of geometrical frustration on a single hole moving in an antiferromagnetic background. We chose the triangular $t - J$ model which at half filling presents a non-collinear magnetic ground state. Using the spinless fermion representation and the self-consistent Born approximation we derived an effective Hamiltonian with two different hole motion mech-

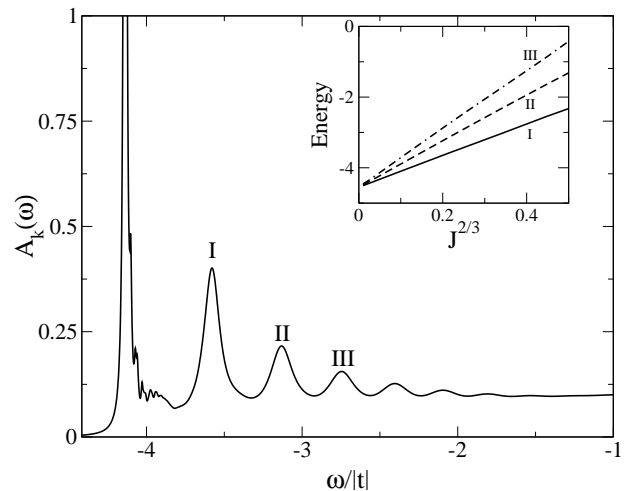


FIG. 6: Spectral functions at the M point for $J/|t| = 0.1$ and negative t . Inset: Energy scaling versus $(J/t)^{2/3}$ of the first three peaks labeled as I, II and III.

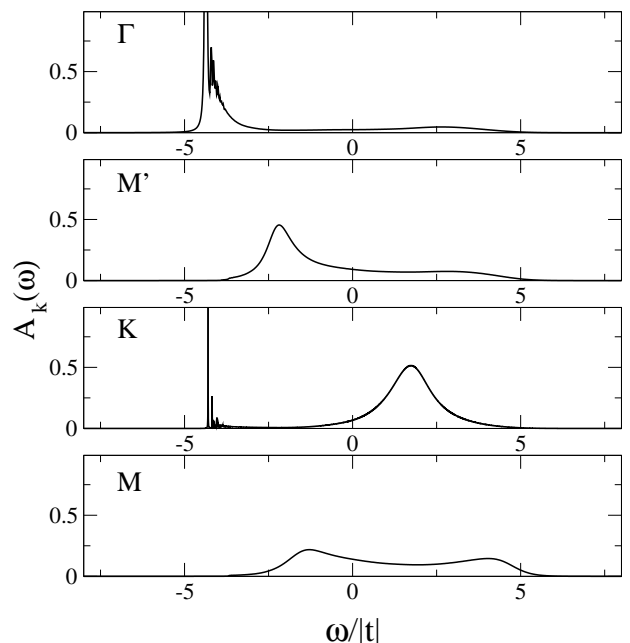


FIG. 7: Spectral function for the Γ , M' , K , M points of the Brillouin zone for $J/|t| = 0.4$ and positive t .

anisms. One of them arises due to spin-flip processes (magnon-assisted) and the other one has its origin from the ferromagnetic components of the non-collinear magnetic order. The latter allows the free hole motion without emission or absorption of magnons and it is absent in collinear antiferromagnets. The reliability of the analytical method (SCBA) is supported by the excellent agreement with the exact diagonalization method on small size clusters.

Unlike previous works^{18,21}, we have performed a detailed description of the whole structures of the spectral function and we were able to trace them back to the two

hole motion processes mentioned above. In particular, we have done a careful analysis of quasiparticles, strings, and free hole resonances in the thermodynamic limit.

We have found new and reliable results of the low energy sector of the spectra. Our main result is the vanishing of the quasiparticle excitation for a *positive* integral transfer t at some momenta and at finite J . Also, we have uncovered other important change of the spectra under t sign reversal: the presence of string-like excitations only for t negative. We suggest that these features are a consequence of different magnetic environment around the hole tuned by the t sign. Based on the quasiparticle energy scaling with J/t , we argue that for negative t the local environment around the hole enhances its AF character, while for the other sign the ferromagnetic character is favored. For small clusters ($N \leq 12$), this behavior is reversed, in agreement with the three-sites problem worked out by Koretsune and Ogata.¹⁰ A deeper study of the magnetic environment using the hole wave function within the SCBA will be presented elsewhere²³.

The dynamics of a hole in the triangular lattice,

for negative t , exhibits the same features of the well known square lattice case^{12,19}: a well defined quasiparticle, string excitations, and antiferromagnetic correlations around the hole. On the contrary, for positive t the dynamics is more irregular: no well defined quasiparticle, no string excitations, and ferromagnetic correlations around the hole.

For decades researchers have tried to look for spin-liquid phases that upon hole doping, give rise to non-conventional excitations¹. Now we give firm evidence that such non-conventional excitations can be found in *non-collinear* spin-crystal phases like the one present in the triangular antiferromagnet.

We acknowledge helpful discussions with A. E. Feiguin, A. Greco, A. Dobry, and D. Poilblanc. A. E. T. thanks the hospitality received at the Universite Paul Sabatier in Toulouse under the PICS France-Argentina 1490. We thank G. Martins for pointing out an error in an earlier version of this manuscript. This work was done under PICT Grant No. N03-03833 (ANPCyT) and was partially supported by Fundaci3n Antorchas.

-
- ¹ P. W. Anderson, *Science* **235**, 1196 (1987); *Phys. Rev. Lett.* **64**, 1839 (1990).
- ² A. Damascelli, Z. Hussain, and Z.-X. Shen, *Rev. Mod. Phys.* **75**, 473 (2003); J. W. Allen, *Solid State Comm.* **123**, 469 (2002).
- ³ R. B. Laughlin, *Phys. Rev. Lett.* **79**, 1726 (1997).
- ⁴ B. O. Wells, Z. -X. Shen, A. Matsuura, D. M. King, M. A. Kastner, M. Greven, and R. J. Birgeneau, *Phys. Rev. Lett.* **74**, 964 (1995).
- ⁵ E. Dagotto, *Rev. Mod. Phys.* **66**, 763 (1994)
- ⁶ R. Coldea, D. A. Tennant, A. M. Tsvelik, and Z. Tylczynski, *Phys. Rev. Lett.* **86**, 1335 (2001).
- ⁷ R. H. McKenzie, *Science* **278**, 820 (1997); *Comments Cond. Mat.* **18**, 309 (1998).
- ⁸ L. I. Johansson, F. Owman, and P. Mårtensson, *Surf. Sci.* **360**, L478 (1996); H. H. Weitering, X. Shi, P. D. Johnson, J. Chen, N. J. DiNardo, and K. Kempa, *Phys. Rev. Lett.* **78**, 1331 (1997).
- ⁹ L. O. Manuel, C. J. Gazza, A. E. Feiguin, and A. E. Trumper, *J. Phys.: Condens. Matter* **15**, 2435 (2003).
- ¹⁰ T. Koretsune and M. Ogata, *Phys. Rev. Lett.* **89**, 116401 (2002).
- ¹¹ M. Ogata, cond-mat/0304405; B. Kumar and S. Shastry, cond-mat/0304210; Q. H. Wang, D. H. Lee, and P. A. Lee, cond-mat/0304377; G. Baskaran, cond-mat/0303649; R. E. Schaak, T. Klimczuk, M. L. Foo, and R. J. Cava, cond-mat/0305450.
- ¹² G. Martinez and P. Horsch, *Phys. Rev. B* **44**, 317 (1991).
- ¹³ D. Poilblanc, H. J. Schulz, and T. Ziman, *Phys. Rev. B* **46**, 6435 (1992).
- ¹⁴ B. Bernu, C. Lhuillier, and L. Pierre, *Phys. Rev. Lett.* **69**, 2590 (1992); L. Capriotti, A. E. Trumper, and S. Sorella, *Phys. Rev. Lett.* **82**, 3899 (1999).
- ¹⁵ L. O. Manuel, A. E. Trumper, and H. A. Ceccatto, *Phys. Rev. B* **57**, 8348 (1998).
- ¹⁶ A. E. Trumper, L. Capriotti, and S. Sorella, *Phys. Rev. B* **61**, 11529 (2000).
- ¹⁷ C. L. Kane, P. A. Lee, and N. Read, *Phys. Rev. B* **39**, 6880 (1989).
- ¹⁸ W. Apel, H. U. Everts, and U. Körner, *Eur. Phys. J. B* **5**, 317 (1998).
- ¹⁹ Z. Liu and E. Manousakis, *Phys. Rev. B* **45**, 2425 (1992).
- ²⁰ P. Béran, D. Poilblanc, and R. B. Laughlin, *Nucl. Phys. B* **473**, 707 (1996).
- ²¹ M. Azzouz and Th. Dombre, *Phys. Rev. B* **53**, 402 (1996).
- ²² F. Lema, Ph.D. thesis, Instituto Balseiro, Bariloche, 1997.
- ²³ A. E. Trumper *et al.*, in preparation.